JGR Oceans

RESEARCH ARTICLE
10.1029/2021JC017209

Climatic Controls on the Spring Phytoplankton Growing Season in a Temperate Shelf Sea

J. E. Jardine[1], M. Palmer[1], C. Mahaffey[2], J. Holt[1], S. Wakelin[1], and Y. Artioli[3]

[1]National Oceanography Centre, Liverpool, UK, [2]School of Environmental Sciences, University of Liverpool, Liverpool, UK, [3]Plymouth Marine Laboratory, Plymouth, UK

Key Points:

- Large-scale climatic oscillations directly impact winter-spring phytoplankton growth rates in NW European shelf seas
- Light is confirmed as a first-order control on spring bloom initiation, which can occur 3 weeks after the onset of seasonal stratification
- Up to 22% of net spring phytoplankton growth occurs before the spring bloom

Correspondence to:
J. E. Jardine,
jenjar@noc.ac.uk

Citation:
Jardine, J. E., Palmer, M., Mahaffey, C., Holt, J., Wakelin, S., & Artioli, Y. (2022). Climatic controls on the spring phytoplankton growing season in a temperate shelf sea. *Journal of Geophysical Research: Oceans*, *127*, e2021JC017209. https://doi.org/10.1029/2021JC017209

Received 29 JAN 2021
Accepted 8 AUG 2021

Abstract The Northwest European Shelf is positioned directly beneath the North Atlantic Storm Track, within which the frequency and intensity of transient storms are modulated by large-scale climatic oscillations. In temperate shelf seas, the impact of storms on the physical environment has received considerable attention, but the effect on biogeochemistry is less studied. Here, we use output from a multidecadal (1982–2015) coupled physical-biogeochemical model supported by observations from ocean gliders to investigate phytoplankton growth throughout the winter-spring transition. We define two separate phytoplankton growth events: the spring bloom, defined as the exponential growth following seasonal stratification, and the prebloom, occurring before stratification, and accounting for up to 22% of the total spring growth. Our results support the paradigm that light is a first-order control, with the spring bloom initiating up to 22 days after stratification onset should light levels be too low to trigger the bloom. The prebloom is heavily influenced by the phase of the Atlantic Multidecadal Oscillation (AMO), demonstrated by an acceleration in the rate of increase of total chlorophyll concentrations (±90% confidence limit) from 7.6 ± 2.8 mg m^{-2} d^{-1} (during a positive AMO) to 13.1 ± 4.3 mg m^{-2} d^{-1} (negative AMO), due to modulation of periods of ephemeral stratification that occur between successive storms. We propose that phytoplankton growth in prebloom events might help buffer the lag between phytoplankton supply and larval recruitment, particularly during years when the spring bloom is delayed.

Plain Language Summary In temperate shelf seas, the seasonal onset of stratification is usually considered the precursor for the spring phytoplankton bloom: an exponential growth of algae that is of key biological importance to fish stocks. Seasonal stratification, whereby the water column becomes layered with warmer water on top of colder water, is initiated by more heat going into the ocean toward spring. Increasing winds, due to passing storms, delay the onset of stratification due to increased mixing. Changes in water temperatures and atmospheric pressure across the North Atlantic change the frequency and intensity of storms across Northwest Europe and influence stratification onset. Using a model that incorporates both physics and biology, we investigated how changing storm patterns from 1982 to 2015 influenced phytoplankton variability during the winter-spring transition. Our results show that the spring bloom is limited by light, and can occur 3 weeks after stratification should light be insufficient for growth. Furthermore, we show that short-lived stratification events throughout the winter period provide high-light oases for phytoplankton growth. These "preblooms," which occur before the onset of stratification, can contribute to over one fifth of the total spring phytoplankton growth and challenges the perception that winter is a biologically unproductive season.

1. Introduction

At temperate latitudes, the onset of the spring phytoplankton bloom is considered light limited, only occurring once cells are contained in the sunlit euphotic zone for prolonged periods. The vertical distribution of phytoplankton is controlled by the depth of the mixed layer (MLD), such that exponential phytoplankton growth is hypothesized to occur once the MLD shoals above a critical depth whereby phytoplankton growth from photosynthesis exceeds net losses from respiration (the Critical Depth Hypothesis; Sverdrup, 1953). This criterion is often met following the onset of seasonal stratification, as this traps phytoplankton near the surface, and is thus considered a precursor to the initiation of the spring phytoplankton bloom.

While some studies still support the Critical Depth Hypothesis (Chiswell, 2011; Siegal et al., 2002), phytoplankton growth observed during the winter months (Behrenfeld, 2010; Boss & Behrenfeld, 2010; Taylor & Ferrari, 2011) casts doubt on the theory's validity. Observations further show that the spring bloom can be initiated before the mixed layer has shoaled above the critical depth (Behrenfeld, 2010; Körtzinger et al., 2008;

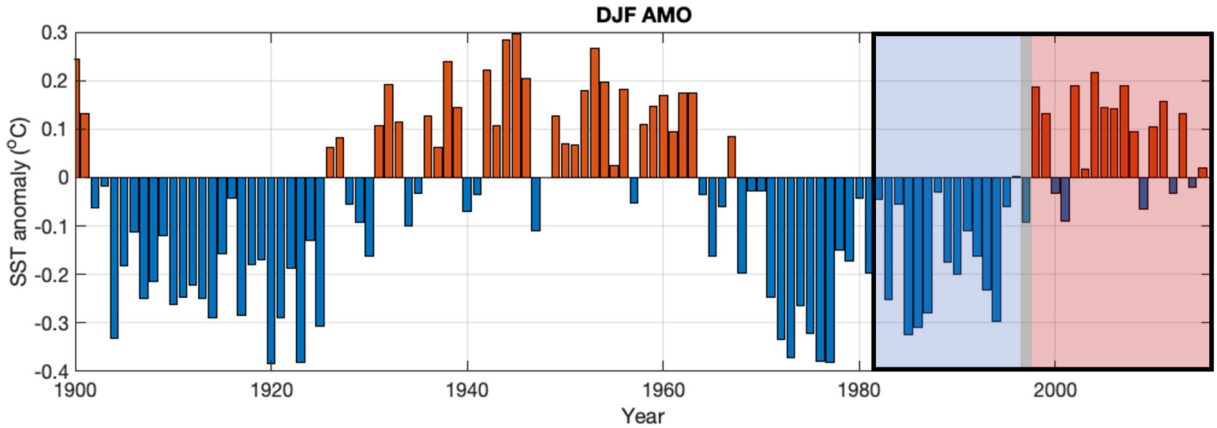

Figure 1. The winter (DJF) Atlantic Multidecadal Oscillation (AMO), as shown by the sea surface temperature anomaly (°C) from 1900 to 2015. The black box, from 1982 to 2015, indicates the time period of the NEMO-ERSEM model data, with the shaded boxes defining the negative (blue) and positive (red) AMO phases, and the transition year (1997). AMO data is the long, unsmoothed series downloaded from https://psl.noaa.gov/data/timeseries/AMO/.

Townsend et al., 1992). Alternative drivers to explain this net pre-stratification phytoplankton growth have been explored, including the recoupling-dilation hypothesis (Behrenfeld, 2010), the shutdown of convective mixing (Taylor & Ferrari, 2011), the shutdown of turbulent controls (Huisman et al., 1999), and local decreases in wind stress (Chiswell, 2011; Chiswell et al., 2013).

On the Northwest European Shelf (NWES), the current paradigm is that the onset of thermal stratification is exclusively dominated by the balance of thermal inputs to wind and tidal stresses (Pingree et al., 1976; Simpson & Hunter, 1974). Storm activity can directly delay the onset of seasonal stratification, and thus the spring bloom initiation, through increased wind stress that homogenizes the water column (Sharples et al., 2006).

The frequency and intensity of storms are modulated by large-scale climate oscillations, such as the Atlantic Multidecadal Oscillation (AMO), which is a mode of natural variability in the North Atlantic (0°–80°N). With an estimated period of ~60–80 years (Alexander et al., 2014; Delworth et al., 2007; Schlesinger & Ramankutty, 1994), the AMO is defined as the temperature anomaly in the North Atlantic and was primarily in a negative (colder) phase from the 1960s until transitioning to the current positive (warmer) phase from the late-1990s (see Figure 1). Another relevant climatic mode is the North Atlantic Oscillation (NAO): a highly variable mode of meteorological variability defined as the difference between the Azores and Icelandic pressure systems (Cohen et al., 2014; Li et al., 2013). The NAO is relatively unstable, exhibiting both intra-annual and decadal variability (Visbeck et al., 2001); however, D'Aleo and Easterbrook (2016) note that an inverse relationship exists between the AMO and NAO at decadal timescales due to ocean-atmosphere interconnectivities. This is emphasized by the NAO exhibiting a more frequently positive phase from 1965 to 1995 (Marshall et al., 2001; Visbeck et al., 2001), followed by a predominantly negative phase since the mid-1990s (Cohen et al., 2014; Li et al., 2013).

The combination of the two climate oscillations directly influences the frequency and intensity of storms transitioning across NW Europe (Figure 2). During positive AMO phases, and thus predominantly negative NAO phases, the increased likelihood of explosive cyclones (Gómara et al., 2012), interspersed with periods of meteorological quiescence due to atmospheric blocking (Häkkinen et al., 2011), has the potential to increase the interannual variability of stratification onset through the formation and destruction of stratification events. Only when mixing from successive storms is insufficient to outcompete the positive buoyancy effects from thermal inputs, will seasonal stratification be initiated and subsequently maintained.

The effect of this climatic control on the timing of the spring bloom remains uncertain. It has been postulated that an increase in storminess might induce a delayed spring bloom response, as increased wind mixing would rapidly transport phytoplankton out of the euphotic zone and limit light availability (Collins et al., 2009; Henson et al., 2006; Sharples et al., 2006; Townsend et al., 1994). However, as both the frequency and intensity of passing storms change with the phase of large-scale climate oscillations (see Figure 2), the effect this has on late winter/early spring phytoplankton phenology remains unknown.

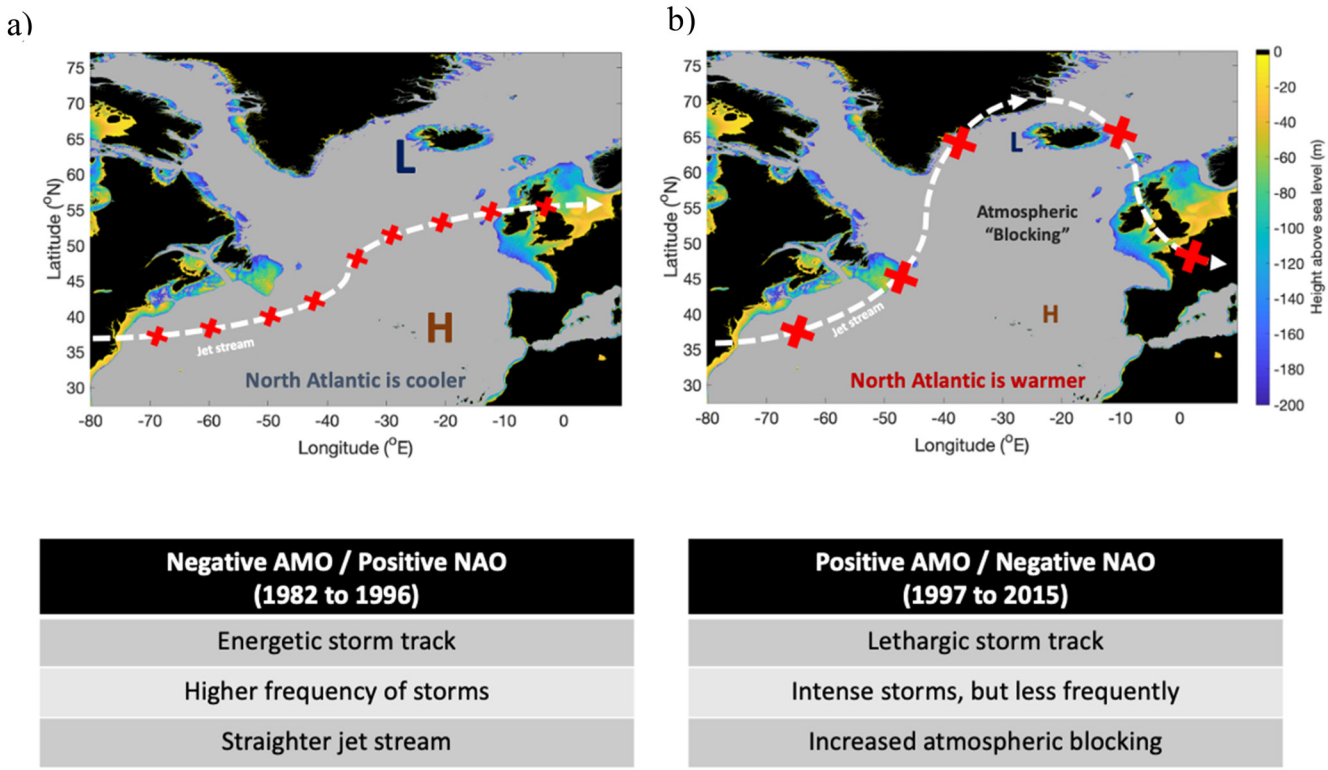

Negative AMO / Positive NAO (1982 to 1996)	Positive AMO / Negative NAO (1997 to 2015)
Energetic storm track	Lethargic storm track
Higher frequency of storms	Intense storms, but less frequently
Straighter jet stream	Increased atmospheric blocking

Figure 2. Schematics detailing the changes of the North Atlantic Storm track, summarized from the main text, with (a) a negative (positive) AMO (NAO) from 1982 to 1996, and (b) a positive (negative) AMO (NAO) from 1998 to 2015. The table in the lower plots summarizes the key changes in storm track characteristics over Northern Europe. The colored sections represent the bathymetry of the continental shelf seas, defined as <200 m deep. Red crosses on the jet stream are indicative of storms; larger crosses are more energetic storms.

To explore the influence of large-scale climatic oscillations on phytoplankton phenology across the winter-spring transition, we quantified the importance of meteorological events on the timing, magnitude, and composition of phytoplankton in the western Celtic Sea, on the NWES. We tied these results to glider observations to lend confidence in our conclusions. Using output from a shelf-sea coupled model, we investigated the effect of these storm systems on the variability of the phytoplankton growing season throughout the winter-spring transition. We further explored the contrasting physical controls that governed phytoplankton variability across the winter-spring, and related them to contrasting phases of the AMO.

2. Materials and Methods

2.1. Model Description

The Nucleus for European Modeling of the Ocean (NEMO) is a model framework that incorporates both ocean dynamics and thermodynamics (Madec, 2015) and was developed from the Océan PArallélisé (OPA) model described by Madec et al. (1997). This was then adapted for use in a shelf sea environment (O'Dea et al., 2012) and on the 7 km Atlantic Margin Model (AMM7; O'Dea et al., 2017) domain before being coupled to the biogeochemical European Regional Sea Ecosystem Model (ERSEM; Butenschön et al., 2016). Details of coupling NEMO to ERSEM can be found in Edwards et al. (2012).

The model domain of AMM7 (Figure 3a) covers the NWES and part of the Eastern Atlantic (20°W, 40°N to 13°E, 65°N). Resolution varies from 9.4 to 5.2 km, resulting in a mean resolution of 7.4 km, and while the resolution is unable to capture the internal Rossby radius (4 km; Holt & Proctor, 2008), this is deemed a justifiable compromise considering the large computer resources needed to run a higher resolution model from 1982 to 2015.

Bathymetry is a combination of GEBCO 1 arcmin data and local data sourced from other partners of the North-west European Shelf Operational Oceanographic System (NOOS). Following the vertical stretching routines

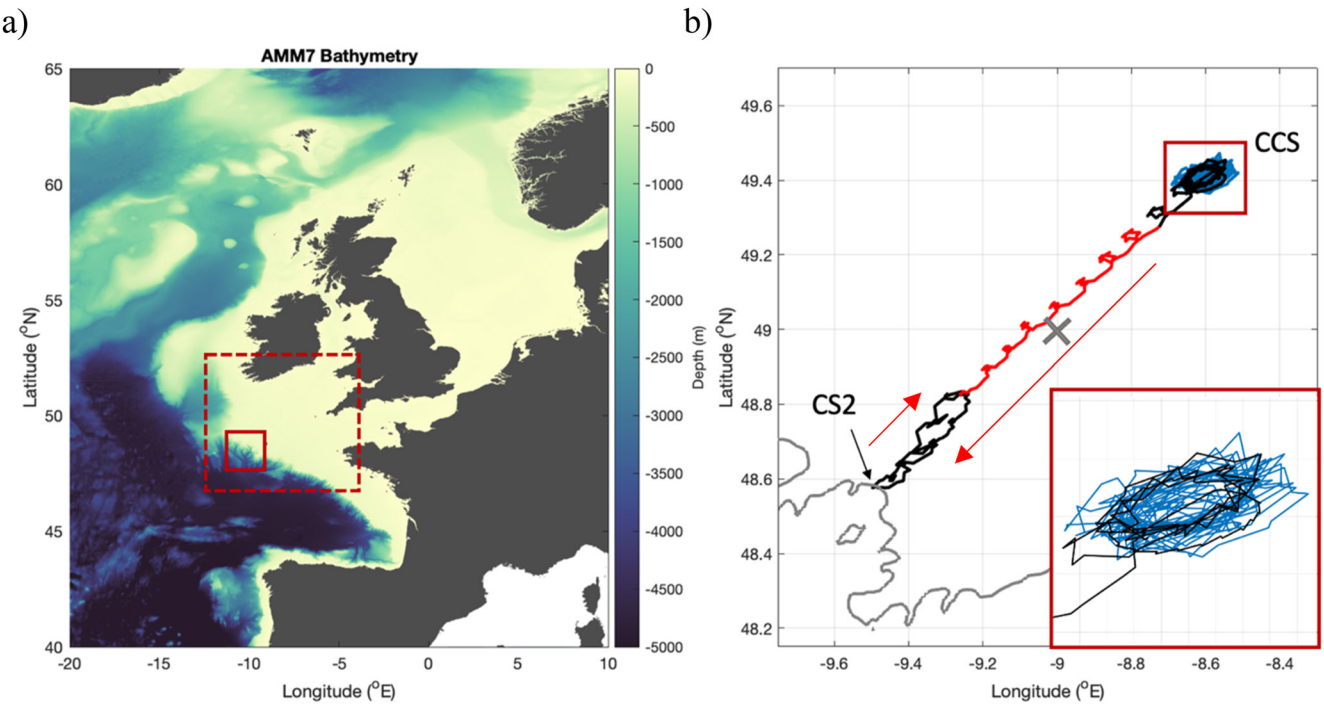

Figure 3. (a) The complete AMM7 domain, with the bathymetry (NOOS) of the shelf and deep ocean (colored) shown (also note the Mediterranean is not included in the AMM7). The red boxes indicate the bounds of Figure 3b (solid box) and the bounds of the shelf for the stratification analysis in Figure 10); (b) Location of the glider track, in relation to the Northwest European Shelf, from March 1, 2015 to April 2, 2015 and consists of two glider tracks: one from March 1 to 22 (blue track) and another glider that ran from March 22 to April 2 (red and black track). The red section of the black track corresponds to a stratification event observed by the glider, from March 25 and 29, and the locations for the Central Celtic Sea (CCS) and the shelf break site (CS2) are also labeled. The gray cross indicates the chosen location for model data analysis and the red arrows indicate the direction of travel. Also included is the 200m isobath (GEBCO, 2014).

of Siddorn and Furner (2013), there are 51 vertical levels that use terrain-following z-σ coordinates (O'Dea et al., 2017). Crucially, vertical levels are uniform near the ocean surface across the whole model domain, allowing for more consistent ocean-air exchanges. River forcing data was sourced from a climatological annual cycle of freshwater discharge, at daily frequency, from the Global River Discharge Database (Vörösmarty et al., 2000). Meteorological and atmospheric forcing data were sourced from ERA-Interim (Dee et al., 2011) and initial conditions and boundary forcing were sourced from the 1/4° ORCA025 hindcast of GO5.0 (Megann et al., 2014). More details of GO5.0's initialization can be found in Ingleby and Huddleson (2007). A full review of the sensitivity tests and validations with observations and previous models (e.g., POLCOMS) can be found in O'Dea et al. (2017).

ERSEM is able to parameterize the complex physiological processes of planktonic and microbial communities within different size classes and functional groups, based on the local stoichiometry and nutrient load of the system (Butenschön et al., 2016; Edwards et al., 2012). Four phytoplankton groups are included in the ERSEM, including microphytoplankton (>20 μm), nanophytoplankton (2–20 μm), and picophytoplankton (<2 μm). The final phytoplankton group is diatoms, as they are the only group able to utilize silicate. A schematic of the pathways and full configurations included in ERSEM are discussed in Butenschön (2016).

2.2. Model Validation

A full sensitivity review and physical validation of the model can be found in Luneva et al. (2019), where biases between the model setup and observations were <0.05°C at the surface and <−0.1°C across the whole model domain. Pycnocline depth exhibited a bias of 5 m deeper for the model compared to observations. For the simulations, Luneva et al. (2019) found that the model skill was very high and satisfactory for SST and pycnocline depth, respectively.

To validate the model for our specific area of interest, we used observational data collected from ocean glider deployments in the Celtic Sea during March 2015 (Jardine et al., 2022), as part of the Shelf Sea Biogeochemistry project (www.uk-ssb.org). The gliders covered a transect of up to 150 km between the Central Celtic Sea (CCS) site and the shelf break (CS2) at a sampling rate of 1 Hz (Figure 3b). The high spatial and temporal resolution of the glider data allowed a qualitative comparison between the onset date of stratification, winter chlorophyll concentrations and the timing of the spring phytoplankton bloom. Glider temperature and salinity profiles from March 25 to 28, 2015 were used to validate the simulated stratification onset in the model, represented by the red part of the transect in Figure 3b, with the model profiles at the closest location to the glider at each model time stamp (see Section 3.1). Further validation of predicted chlorophyll was provided during April and May 2015 (which included the peak of the spring bloom), when the magnitude of depth-integrated modeled chlorophyll concentrations was comparable to bottled samples collected on nearby process cruises (Poulton et al., 2019).

2.3. Defining the Onset of Stratification, Prebloom, and Spring Bloom

The potential energy anomaly, ϕ (J m^{-3}; Simpson & Bowers, 1981), representing the amount of mechanical energy needed to vertically mix the water column between the sea surface and the seabed, provides a measure of stratification in shelf seas. The strength of stratification can be measured by ϕ, with a well-mixed water column having ϕ equal to 0 and increasing positive ϕ representing increasing stratification. Negative ϕ in the model indicates static instability, which is very rapidly mixed (see Holt & Umlauf, 2008). Homogeneous water columns have small positive values of ϕ and as such, the onset of seasonal stratification in the model was therefore defined as the last date before summer when $\phi < 2$ J m^{-3}.

Modeled chlorophyll concentrations were analyzed according to the onset of the prebloom and spring bloom. The onset of the phytoplankton prebloom period was defined as when the rate of increase in surface (0–10 m) chlorophyll concentrations first exceeded 0.01 mg m^{-2} d^{-1}, and was used to identify the start of gradual phytoplankton growth following the unproductive winter period and lasted until the initiation of the spring bloom. The onset of the spring bloom was defined as the first date when the rate of increase in surface (0–10 m depth) chlorophyll concentrations exceeded 0.15 mg m^{-2} d^{-1} consistently for 5 days and was used to identify the exponential increase in phytoplankton biomass that is characteristic of the spring bloom. This definition is bespoke to this study, as we defined the spring bloom as only occurring after the onset of seasonal stratification, with any phytoplankton growth before this being defined as the prebloom (see Section 3.2). Other available definitions for the onset of the spring bloom, such as those suggested by Siegal et al. (2002), do not seek to distinguish between these two periods of phytoplankton growth, and so were not considered for this study.

To assess the climatological explaining factor for the phytoplankton prebloom and spring bloom periods, the AMO was used as the main climatological driver of winter-spring phytoplankton phenology because it is a more stable indicator compared to the NAO. The negative (or cooler) AMO phase occurs from 1982 to 1996, with the positive (or warmer) AMO phase from 1998 to 2015 (Figure 1). Stratification was anomalously early in 1997 (February 26) compared to 34-year average (April 4) and 1997 was thus was excluded from the AMO phase analysis. However, we still used 1997 as a case study year to investigate the timing of the spring bloom in relation to an anomalously early onset of stratification (see Section 3.2).

3. Results

3.1. Model Validation

The model adequately replicated the spatiotemporal variations in both the temperature and salinity depth-meaned anomalies. Temperature anomalies were represented well in the model (Figures 4a and 4b), with consistent maximum and minimum values, yet some of the more subtle switches in positive and negative surface temperature anomalies were not captured, possibly due to the 3-hourly resolution of the meteorological forcing.

For salinity (Figures 4c and 4d), the model captured the initial surface decrease in salinity anomalies, accurately mixing it to a similar depth recorded in the glider data, around 65 m, with alternating positive and negative salinity anomalies well represented throughout the time period. There was only a 3-hr offset between the initial decrease in surface salinity on March 25, 2015, likely from discrepancies between the modeled and observed precipitation timing (e.g., ERA-I data has a 3-hr frequency) or the spatial resolution of the model grid. We can be

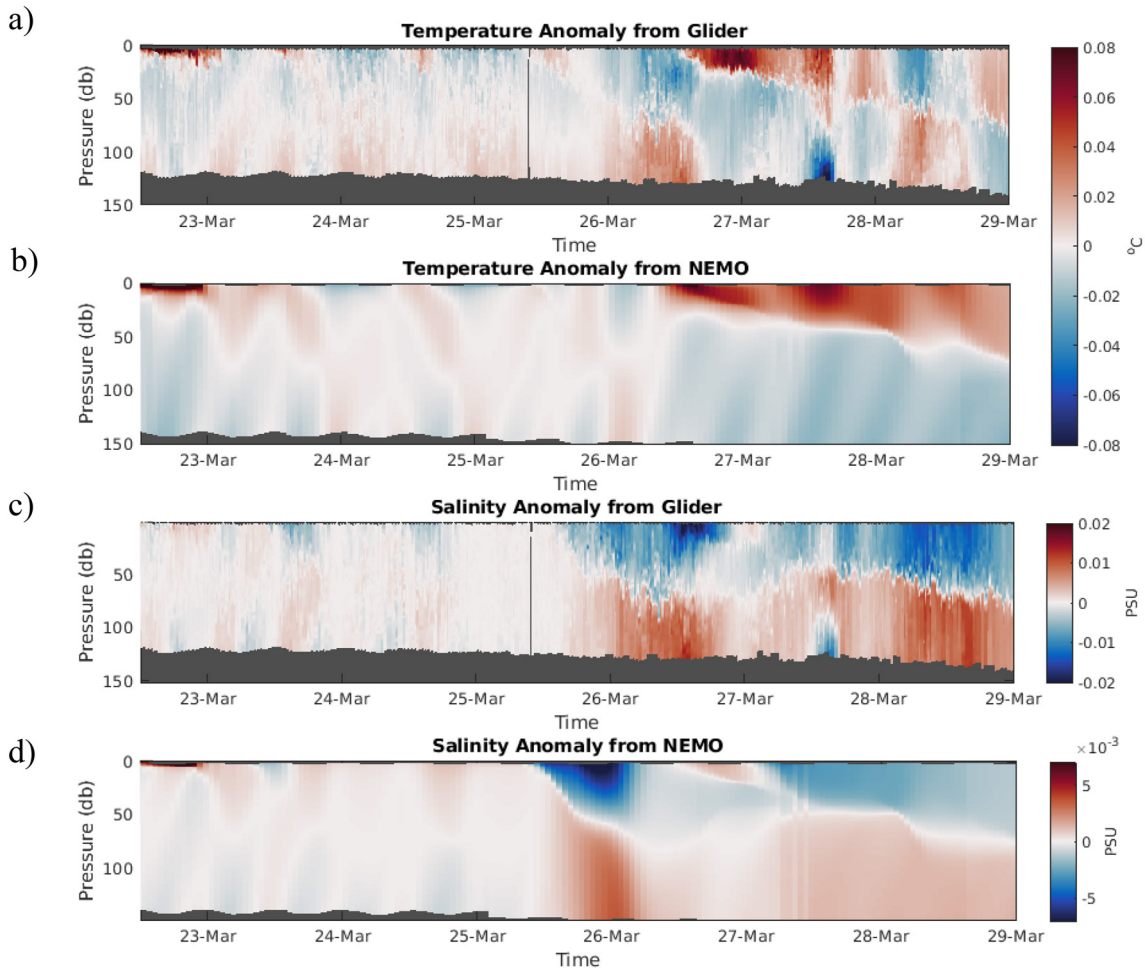

Figure 4. Comparisons of glider (a) temperature and; (b) salinity anomalies to NEMO (c) temperature and; (d) salinity anomalies at the closest location to the glider, from March 22 to 29, 2015 (covering the initial onset of seasonal stratification). Note the differences in scale between the temperature and salinity plots, as due to discrepancies between the data, it was necessary to plot the salinity anomaly for the model and glider data on slightly different color axes.

confident that both the timing of stratification and smaller-scale variations close to the sea surface, resulted from episodic meteorological events and were adequately replicated in the model. While there was good agreement in the patterns, salinity anomalies in the model were typically two times lower than those observed by the glider.

Chlorophyll concentrations from the glider (determined by chlorophyll fluorescence) and the model were compared in Figure 5. The vertical and spatiotemporal distribution of chlorophyll concentrations were replicated in the model, such as on March 28, where surface chlorophyll concentrations were gradually mixed to a depth of 100 m. Before the onset of stratification, observations were limited with data gaps from March 11 to 20, 2015, due to technical failures in the glider (i.e., gray gaps in Figure 5a), yet a relative increase in chlorophyll concentrations at depth, from March 10 to 22, was captured in both observations and model data. Despite the lack of glider data, enhanced surface chlorophyll was likely redistributed throughout the water-column, following the erosion of ephemeral stratification events that formed between March 8 and 13, 2015. However, there was a clear disparity in the bottom mixed layer between March 26 and 28, where more chlorophyll was seen at depth in the model, likely due to enhanced mixing toward the shelf break. Comparing the modeled chlorophyll concentrations to bottled samples, collected on nearby process cruises (Poulton et al., 2019; Figure 6), showed that the maximum integrated chlorophyll differed by 23 mg m^{-2} between model (175 mg m^{-2}) and observations (152 mg m^{-2}), the shape of the spring bloom was consistent. However, the timing of the spring bloom occurred 9 days later in the model compared to observations (Poulton et al., 2019).

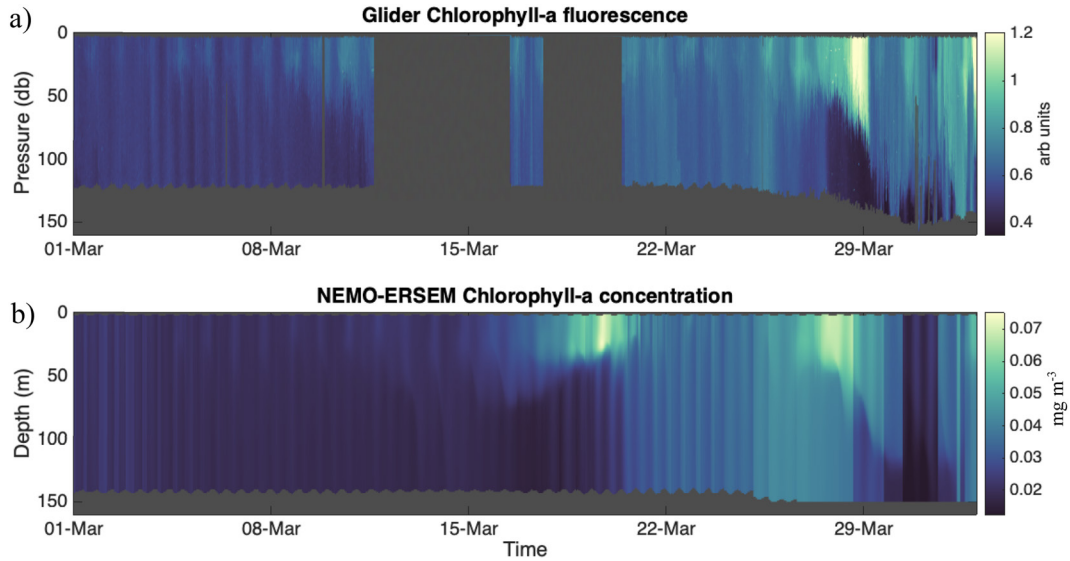

Figure 5. (a) Chlorophyll fluorescence measured from the glider; and (b) chlorophyll concentrations from the AMM7 NEMO-ERSEM model at the closest location to the glider. The gray gaps at the bottom of the figures indicate missing data due to the seabed, while the vertical gray gaps represent missing data due to technical failures in the glider.

3.2. Spatial Phytoplankton Variability

Phytoplankton patchiness (e.g., Martin, 2003) was reproduced in the model (e.g., see Figure 7). Daily depth-integrated chlorophyll concentrations for the shelf break (SB), the inner shelf (CCS) and two mid-point locations (as shown in Figure 7), named X_1 and X_2 and located 52 and 66 km from the shelf break, respectively, are shown in Figure 8. Despite the distance between the shelf break and CCS model points (125 km), there was little variation in the timing of the spring bloom. Instead, there was a 4.5-day offset in bloom initiation at X_1 and X_2 compared to the model output for CCS (Figure 8) and could explain the disparity between modeled and observed chlorophyll observations in Figure 6. While the timing of the spring bloom initiation at X_1 and X_2 differed by only 7 hr, there were differences in the evolution of their respective spring blooms, as shown by the chlorophyll concentrations. The magnitude of chlorophyll concentrations was similar at X_1 and X_2 on April 21, but diverged to a maximum difference of 47 mg m^{-2} by May 3, despite being relatively close (14 km). Chlorophyll concentrations at X_1, X_2, and the CCS site converged and stabilized from May 23, 2015, suggesting a spatial homogenization of phytoplankton across the region.

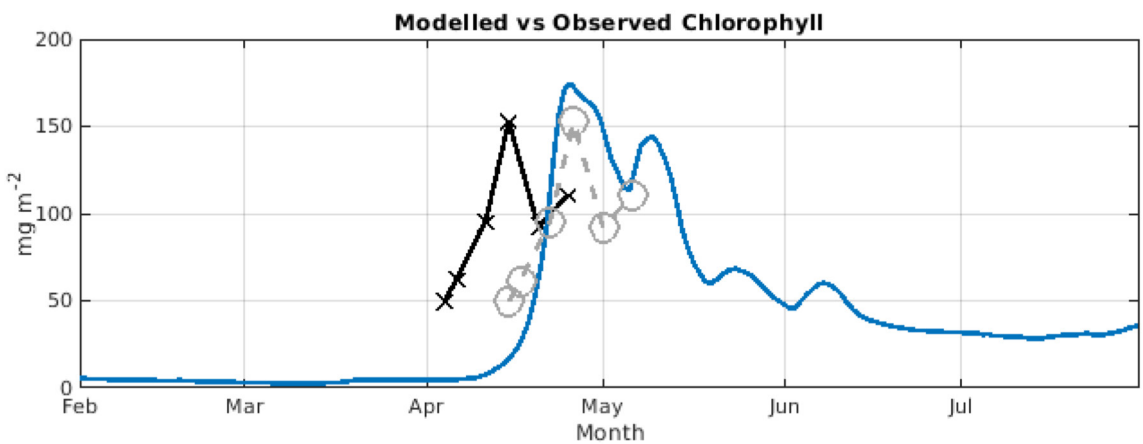

Figure 6. Comparison of the depth-integrated total chlorophyll concentrations (mg m^{-2}) from the AMM7 NEMO-ERSEM model at the CCS site (blue line), with observed depth-integrated chlorophyll concentrations (mg m^{-2}), measured at CCS throughout 2015 (black line; Poulton et al., 2019). The gray line/circles are the CCS observations shifted later by 9 days, to coincide with the peak spring bloom simulated in the model.

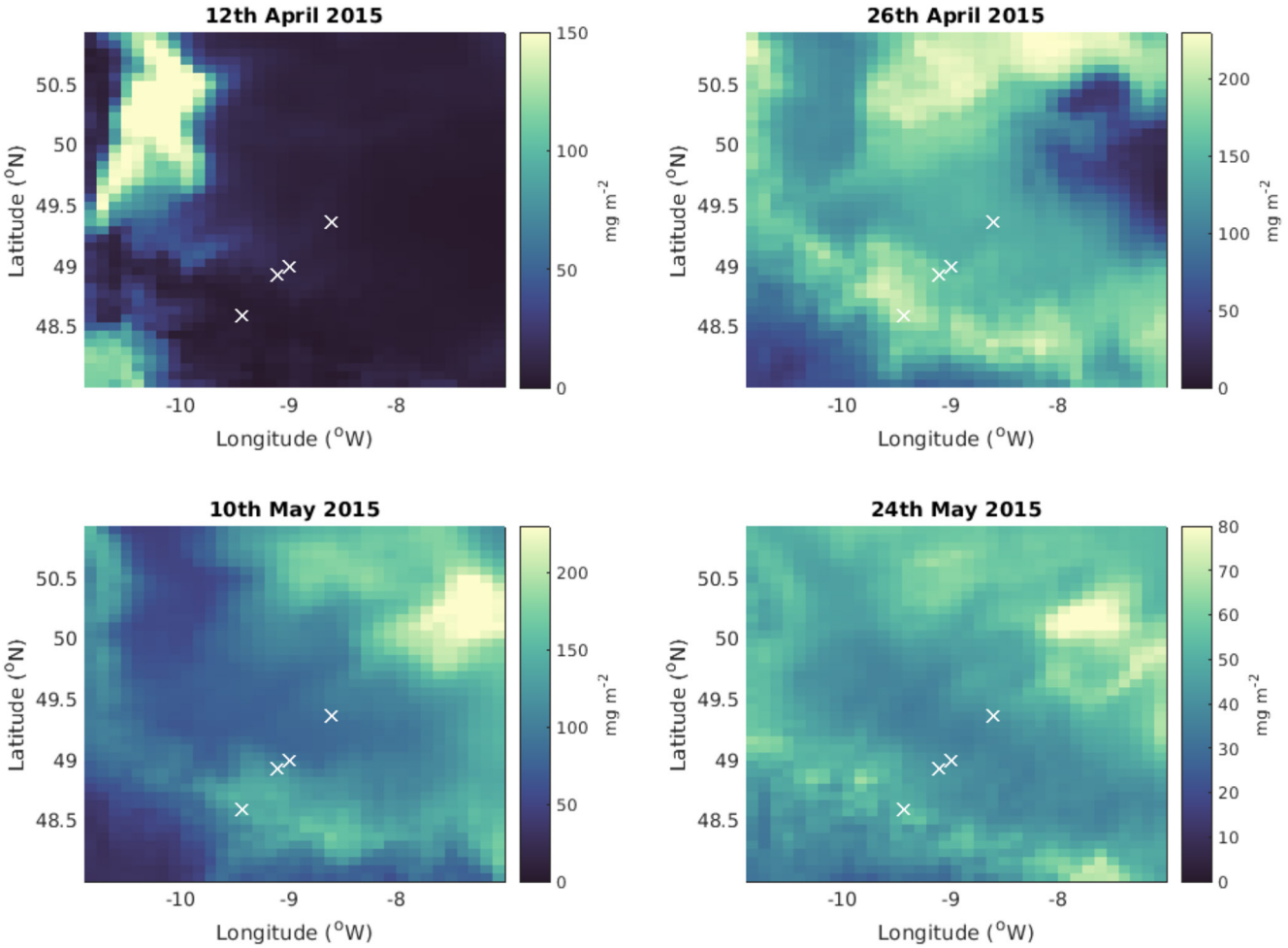

Figure 7. Example plots of depth-integrated chlorophyll concentrations from the NEMO-ERSEM model, demonstrating the degree of phytoplankton patchiness. Note the scales are different for each plot. The white crosses are the locations of the four virtual moorings, as discussed in the main text and in Figure 8, and labeled (from bottom left to top right) as follows: SB (shelf break), X_1, X_2, and CCS (Central Celtic Sea).

While the model was unable to capture the exact timing of the spring bloom, it did capture the physical preconditioning and the evolution of the bloom itself. Thus the model was used to explore the interannual variability in bloom formation and relative timing rather than the exact date of the onset. So, while this study does not investigate the exact date of bloom initiation, the model was suitably used to investigate the interannual variability in the relative timing of the spring bloom. To remove the impact of spatial inhomogeneity of the system, analysis of the model data focused on a single location (49°N, −9°E; shown by the gray cross in Figure 3b), that corresponded to the onset of seasonal stratification observed by the glider on March 25, 2015, and was also away from the shelf break to capture the reaction of a typical on-shelf environment to hydro-climatic forcing.

3.3. Winter-Spring Phytoplankton Variability

Analysis of the model results demonstrated that the mean spring bloom initiation occurred 7 days earlier during positive AMO periods compared to negative AMO periods (statistically significant at 90% confidence; Figure 9a). As seasonal stratification is often considered a precursor for spring bloom initiation in temperate shelf seas (e.g., Franks, 2015; Pingree et al., 1976; Sharples et al., 2006, 2013), we compared the onset of seasonal stratification across the whole Celtic Sea region (Figure 10). This demonstrated a 9.2-day shift to earlier seasonal stratification onset between negative and positive AMO phases. While exploring the biogeochemical response across the entire shelf is outside the scope of this work, the strong positive correlation between the onset of seasonal stratification and the initiation of the spring bloom ($R = 0.85$ and $p \leq 0.0001$) in Figure 9c demonstrates that the discussed

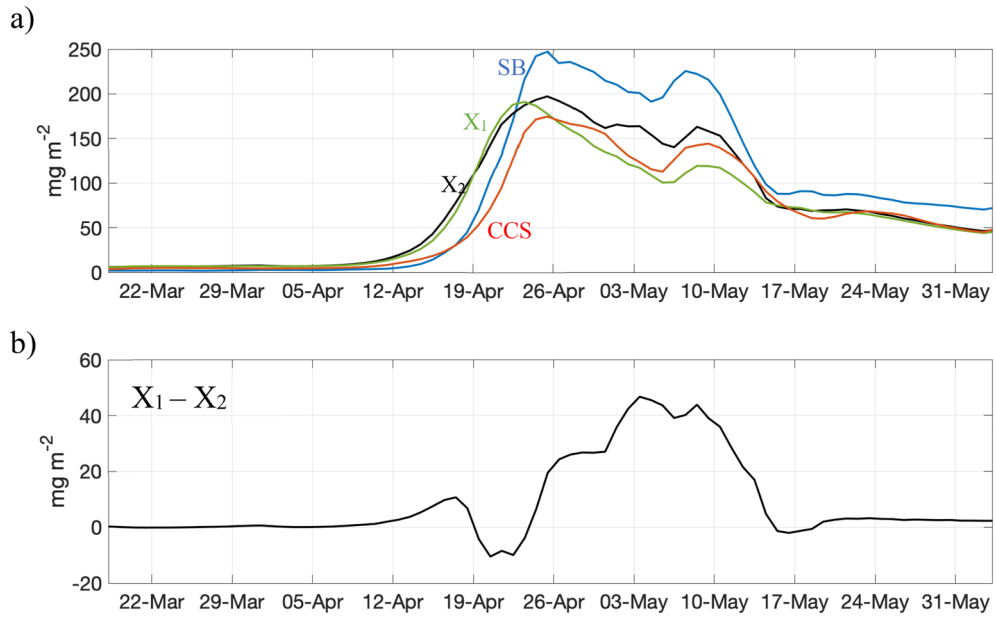

Figure 8. (a) Depth-integrated chlorophyll concentrations (mg m^{-2}) from the AMM7 NEMO-ERSEM model during 2015, at four different locations: the shelf break (SB; blue), the inner shelf (CCS; red) and two mid-point locations located 52 km (X_1; green) and 66 km (X_2; black) from the shelf break; and (b) the black line shows the difference in chlorophyll concentrations between the X_1 and X_2 sites.

biogeochemical responses to stratification are still applicable across much of the outer shelf region of the Celtic Sea.

Further analysis revealed a time lag between the onset of seasonal stratification and the initiation of the spring bloom during both positive and negative AMO phases (dotted line in Figure 9c). For example, the earliest stratification onset occurred on February 26, 1997, with the spring bloom initiating 22 days later, and contrasted to an immediate spring bloom initiation following a much later seasonal stratification onset date of April 30, 2012.

Out of the 34 years, 47% of the prebloom periods occurred after the onset of seasonal stratification (Figures 9b and 9d, green dots), implying slow development of the spring bloom, and further displayed a strong correlation to the onset of seasonal stratification ($R = 0.97$; $p \leq 0.0001$). However, the remaining 18 preblooms occurred before the onset of seasonal stratification (Figure 9d, blue dots, $R = 0.41$; $p = 0.09$). As they occur before the onset of seasonal stratification, only these 18 prebloom periods will be included in further analysis.

Prebloom duration was 6.8 days longer during positive AMO periods compared to negative AMO periods (Figure 11a). The rate of increase in total depth-integrated chlorophyll concentrations within the prebloom period, normalized relative to the length of the prebloom (in days), exhibited a statistically significant (at 90% confidence) increase between negative and positive AMO phases (Figure 11b) from 7.6 ± 2.8 to 13.1 ± 4.3 mg m^{-2} d^{-1}.

3.4. Case Study: Early Seasonal Stratification, 1997

From February 20 to 25, 1997, a low-pressure system caused windspeeds of between 13.9 and 18.1 ms^{-1} that would have promoted the mixing of the upper water column, inhibiting the formation of stratification (Figure 12). Stratification ultimately occurred on February 26, 1997; however, a lag was observed between the onset of stratification (represented by ϕ) with the initiation of the spring bloom. Initial phytoplankton growth did not occur until March 10, 1997, with the spring bloom occurring on March 20, 1997, 22 days after the onset of seasonal stratification. As stratification is already present, phytoplankton cells would be contained in the upper water column, suggesting that light-limited phytoplankton growth.

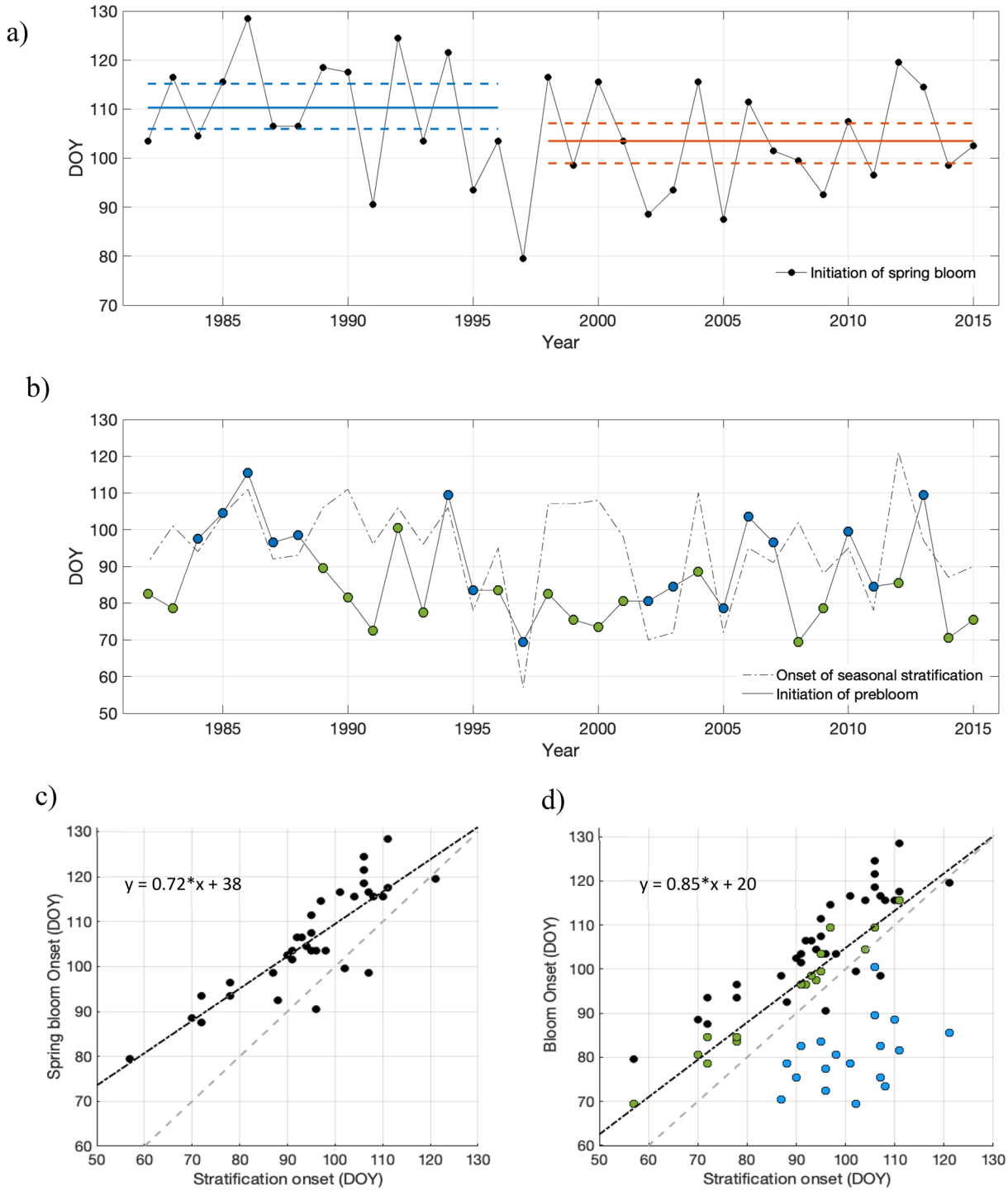

Figure 9. (a) Year day for the onset of the spring bloom (black line) from 1982 to 2015. The mean spring bloom onset (solid colored lines) and the 90% confidence limits (dashed colored lines) are labeled for the negative AMO period (blue) and the positive AMO period (red); (b) Year day for the onset of seasonal stratification (gray dashed line) from 1982 to 2015, as well as the onset days for the prebloom (solid line). The preblooms that initiate before the onset of seasonal stratification are shaded blue, and those that occur after are shaded green; (c) Onset day of seasonal stratification compared to the onset date of the spring bloom (black dots). The dotted lines are a linear regression (black), as well as a 1 to 1 line for reference (gray); (d) The onset day of seasonal stratification compared to the onset date of the spring bloom (black dots) and prebloom (colored dots). The dotted lines are a linear regression of the black and green dots (black), as well as a 1 to 1 line for reference (gray). The colored dots for the preblooms initiations are labeled as those that initiated before (blue) and after (green) the onset of seasonal stratification.

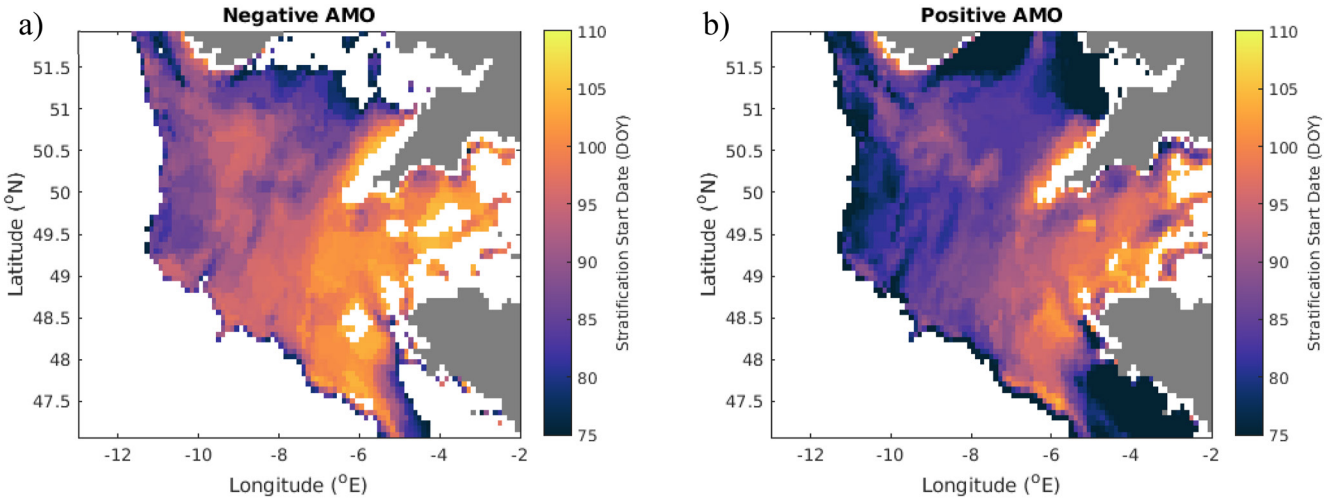

Figure 10. Seasonal stratification onset date in the AMM7 model for the whole of the Celtic Sea shelf for (a) negative AMO; and (b) positive AMO period. The white spaces are indicative of a water depth of >200 m (to distinguish the shelf region) or where the start dates are outside of 75 or 110 (to remove the influence of well-mixed coastal regions). The gray regions are land points in the model.

Total surface photosynthetically active radiation, PAR (sourced from ERA-Interim; Dee et al., 2011) from January to March 1997 was the lowest throughout the 34-year study period (Figure 13). This variation in light was due to an average of 74% cloud cover in February 1997 and 70% in March 1997 (Figure 13c). In contrast, there was higher cloud cover in February 1986 (91%) and February 2012 (86%), but stratification occurred 2 months later, on April 21, 1986 and April 30, 2012, respectively, when the seasonal increase in light and reduced cloud cover produced favorable conditions for phytoplankton growth.

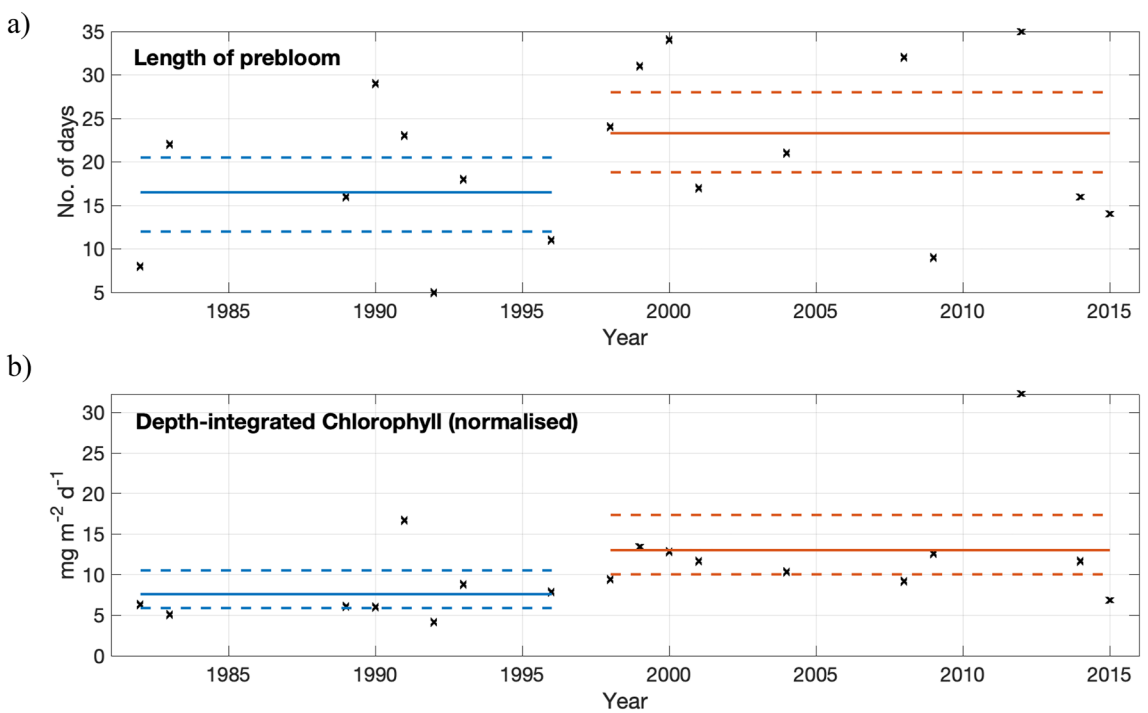

Figure 11. (a) The length of the prebloom period in number of days (black crosses), and (b) the depth-integrated chlorophyll concentration (mg m^{-2}) from AMM7 NEMO-ERSEM, normalized to the length of the prebloom (in days). In both (a) and (b), the mean (solid lines) and the 90% confidence limits (dashed lines) have been included for the negative (blue) and positive (red) AMO phases.

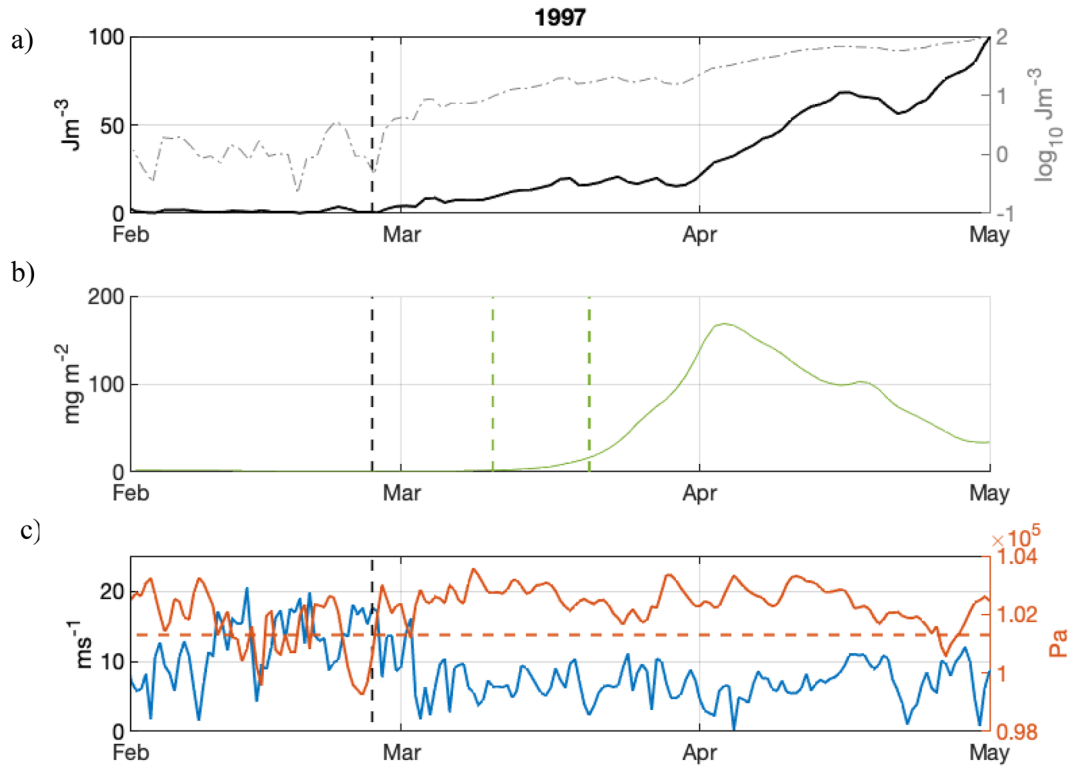

Figure 12. (a) Potential energy anomaly (ϕ, J m^{-3}) from February to May 1997 (black line), including ϕ on a log scale (gray line); (b) the depth-integrated chlorophyll concentration (mg m^{-2}) with the initial and exponential phytoplankton growth indicated by the vertical green dashed lines; (c) the 10 m wind speed (ms^{-1}, blue) and surface air pressure (Pa, red), with the red dashed line indicating standard sea level pressure (as defined by the Met Office). In all plots, the onset of seasonal stratification is labeled by the vertical dashed black lines. Source of meteorological data: ERA-Interim (Dee et al., 2011).

3.5. Case Study: Delayed Seasonal Stratification, 2012

The physical drivers of the prebloom events can be further explored by considering 2012 as a case study. In direct contrast to 1997, 2012 experienced the latest stratification onset out of the 34-year study period (see Figure 9b), occurring on April 30, 2012. Furthermore, a period of ephemeral stratification occurred between March 19 and April 5 that coincided with a prebloom phytoplankton growth event (Figure 14). This stratification was later broken up by a series of storms with wind speeds of up to 20 ms^{-1}. Seasonal stratification ultimately occurred on April 30, 2012 as wind speeds decreased to 8.6 ms^{-1}.

The 2012 prebloom event was the largest out of the 34-year study period and accounted for 17% of the total prebloom chlorophyll concentrations, and 22% of the entire 2012 spring phytoplankton growing season. The 2012 prebloom was initiated on March 25, 2012 and coincided with an increase in ϕ from 3.5 to 23.3 J m^{-3} over 8 days. Chlorophyll concentrations further increased from 24 to 84 mg m^{-2}, despite water column homogenization, over the 30 days before the onset of seasonal stratification.

In direct contrast to 1997, total PAR levels from January to March 2012 were in excess of the standard deviation from the mean (Figure 13a). Furthermore, average cloud coverage reduced from 86% in February to 56% in March (Figure 13c), the lowest March cloud coverage in this study.

4. Discussion

Models predict an earlier onset of seasonal stratification on the NWES in the future (Holt et al., 2010; Sharples et al., 2013), implying an earlier initiation of the spring bloom. However, the multidecadal analysis here shows that this may not be the case and suggests decoupling between the onset of seasonal stratification and the onset of

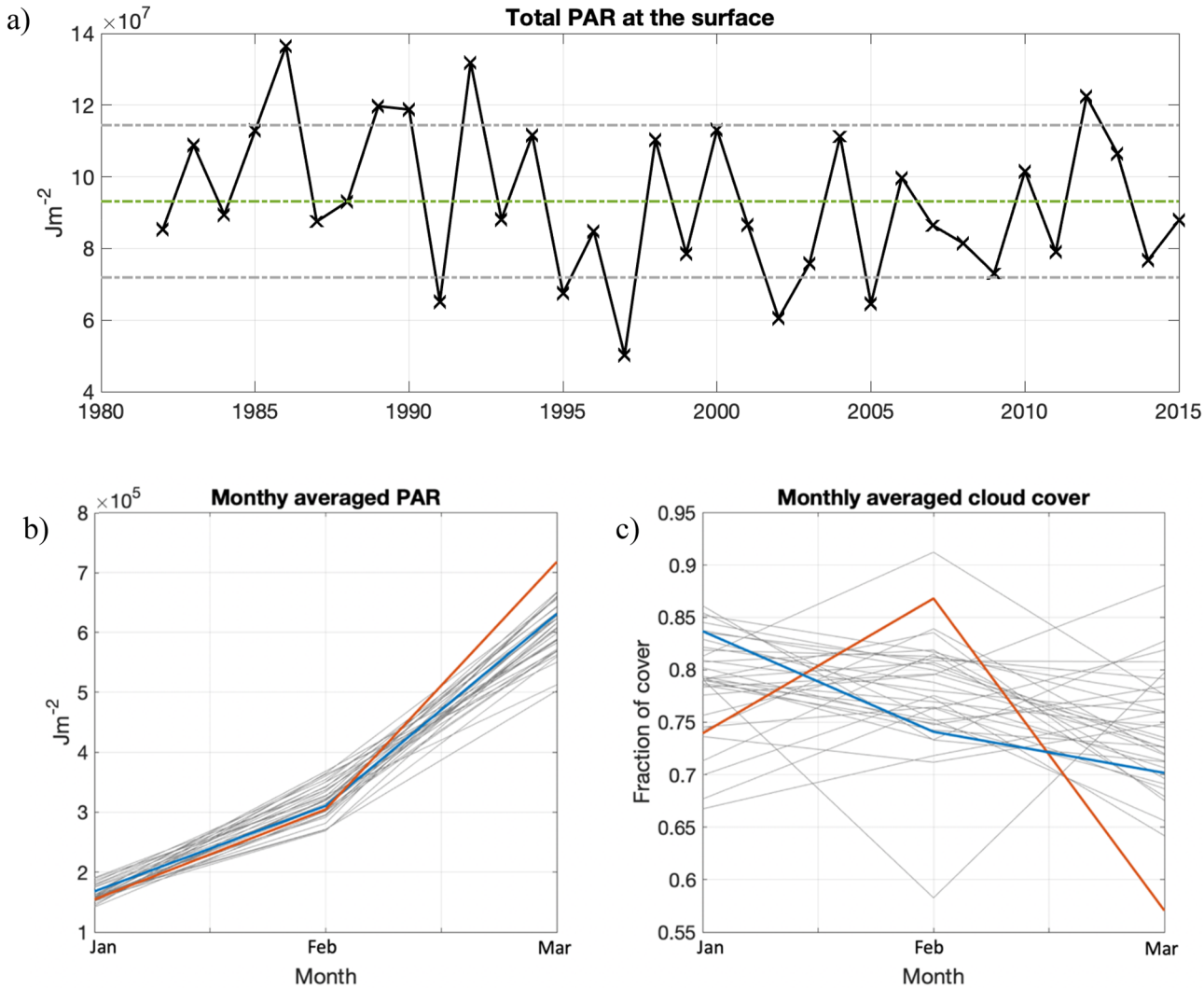

Figure 13. (a) The total January–March photosynthetically active radiation (PAR; J m^{-2}) from 1982 to 2015, where the green dotted line is the mean, and the gray lines are the standard deviations from the 33-year mean; (b) monthly averaged PAR for January, February, and March for each year between 1982 and 2015 (gray lines); and (c) the average fraction of cloud cover for January, February, and March for each year between 1982 and 2015 (gray lines). In (b) and (c), 1997 and 2012 are labeled as the blue and red lines, respectively. Data downloaded from ERA-Interim (Dee et al., 2011).

spring phytoplankton growth. These results are consistent with mesocosm experiments by Sommer and Lengfellner (2008), who found that light was more critical than temperature for spring bloom initiation.

Independent studies by Weisse et al. (2005) and Krueger et al. (2019) indicate increased storminess across the northeast Atlantic from the 1960s to the 1990s, with the annual averaged 99th percentile of geostrophic wind speed (1870–2016) increasing from −0.5 in 1960 to 1.98 in 1990, before decreasing to −1.7 in 2010 (Kreuger et al., 2019). During the negative AMO phase from 1982 to 1996, a higher frequency of storms, as noted by Weisse et al. (2005) and Krueger et al. (2019), acted to mix the water column and was characteristic of winter shelf sea conditions. By contrast, after 1995 during the positive AMO phase, a lower number of cyclones combined with atmospheric blocking resulted in periods of ephemeral stratification that promoted localized phytoplankton growth, occurring before the onset of seasonal stratification.

Phytoplankton growth can occur within these winter/spring prebloom periods if light is sufficient. Lower levels of PAR, modulated by cloud cover, can delay phytoplankton growth. For example, we postulate that the anomalously late spring bloom initiation, related to the onset of seasonal stratification, in 1997 was due to an unfavorable light environment for phytoplankton growth, despite the anomalously early onset of stratification on February

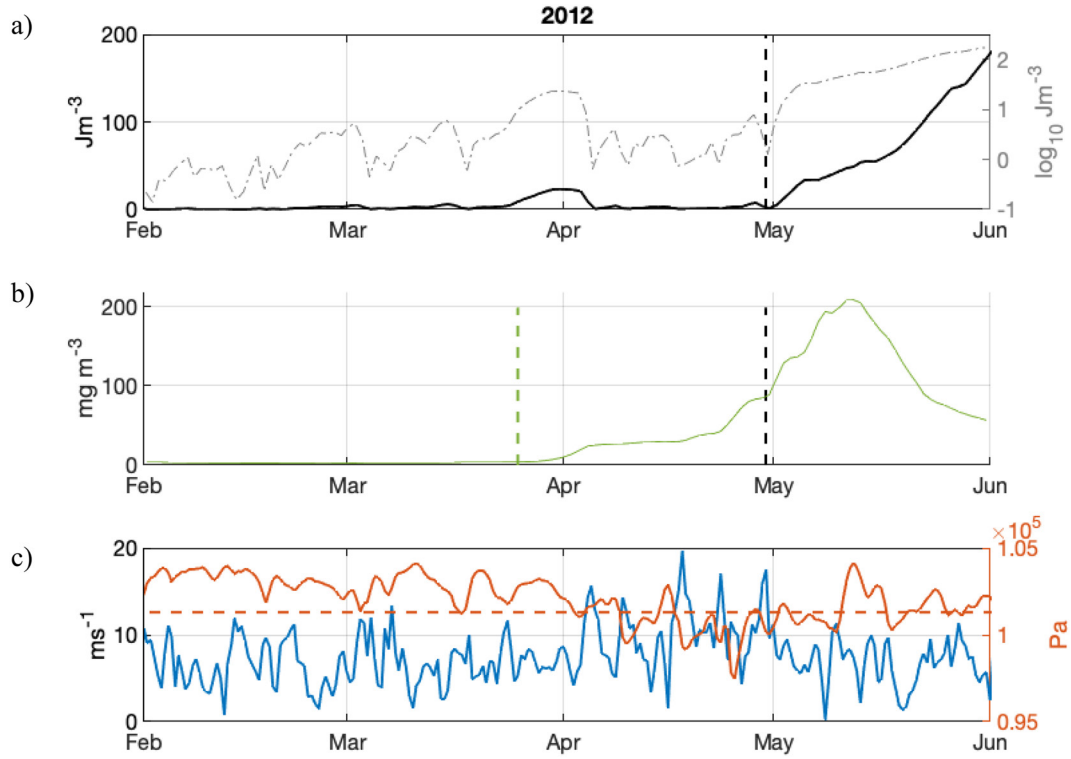

Figure 14. (a) Potential energy anomaly (ϕ, Jm^{-3}) from February to May for 2012 (black line), including ϕ, plotted on a log scale (gray line); (b) the depth-integrated chlorophyll concentration (mg m^{-2}) with the onset of the prebloom indicated by the vertical green dashed line; and (c) the 10 m wind speed (ms^{-1}, blue) and surface air pressure (Pa, red), with the red dashed line indicating standard sea level pressure (as defined by the Met Office); The onset of stratification (vertical black lines) are also added. Source of meteorological data: ERA-Interim (Dee et al., 2011).

26, 1997. In contrast, the low cloud cover (56%) during March 2012, combined with stratification events occurring relatively late in the year where incident light was higher, provided a suitable environment for phytoplankton growth, resulting in the largest prebloom of the study period. These prebloom phytoplankton populations eventually formed the seed populations in the spring bloom, once seasonal stratification was established.

Many marine organisms synchronize their spawning cycles with the occurrence of the spring bloom (Cushing, 1974; Platt et al., 2003), ensuring larvae have an ample food source. An increase in spring bloom variability, such as observed during positive AMO periods, will likely exacerbate the mismatch between phytoplankton abundance and larval production (Cushing, 1974, 1990; Durant et al., 2007). In contrast, longer, more productive prebloom periods may act to buffer this mismatch, by promoting sustained phytoplankton growth before the spring bloom has been initiated, as long as there are sufficient nutrients supplied.

The cumulative amount of carbon fixed during several short-lived winter stratification events in the North Atlantic, resulting in localized increases in diatom populations, has been postulated to make significant contribution to annual carbon export to the deep ocean by downward particle flux and remineralization (Lacour et al., 2017). Despite a similar series of ephemeral stratification events, with subsequent localized phytoplankton blooms, the carbon export observed by Lacour et al. (2017) is unlikely to occur in shelf seas, given that the water column quickly homogenizes after each seasonal stratification period. However, a gradual increase in phytoplankton standing stock occurring directly before seasonal stratification, such as occurred in 2012, could still boost carbon fixation even before the onset of the spring bloom. While the SSB project concluded that carbon is not exported from the Celtic Sea shelf on an annual basis, the consistent seasonal carbon deficit infers an intermittent flux of carbon from the shelf into the deep ocean (Sharples et al., 2019), and a boost in phytoplankton growth before seasonal stratification may be an overlooked contributor to this carbon sink.

Storm number and intensity, and high-wind events across NW Europe are hypothesized to increase with future climate change (Mölter et al., 2016) and could lead to an increased occurrence of prebloom periods before the

onset of seasonal stratification. Increased anthropogenic warming could prolong ephemeral stratification events by increasing the net heat flux into the ocean, lengthening the productive prebloom periods that occur before the onset of seasonal stratification. Such elevated preblooms would directly feed into the higher trophic levels, through the availability of food for larval recruitment, as well as preconditioning the spring bloom community succession and enhancing winter-spring carbon fixation (providing there are sufficient nutrients). With marine air temperatures around the UK increasing at a rate of 0.2–0.4°C decade^{-1} (Dye et al., 2013), ephemeral stratification events during late winter and early spring could become more frequent in the future, suggesting that the processes occurring during the warmer (positive) AMO phase studied here could be considered analogous to future climate conditions.

5. Conclusions

Through the use of a coupled hydrodynamics-ecosystem model validated using high-resolution data from an ocean glider, we have demonstrated how large-scale climatic oscillations in the North Atlantic directly impact the productivity of a temperate shelf sea in winter-spring. We showed that phytoplankton growth, occurring before the onset of seasonal stratification, significantly increased from negative to positive AMO periods and this can be attributed to the meteorological control of prebloom formation and destruction. This work emphasizes that the intrinsic links between ocean-atmosphere coupling are crucial for predicting how ecosystem functioning will respond to future anthropogenic warming.

Conflict of Interest

The authors declare no conflicts of interest relevant to this study.

Data Availability Statement

SSB NEMO-ERSEM data is currently stored and available on the Jasmin supercomputer.

Acknowledgments
This research was funded through the EAO NERC-DTP, in conjunction with the University of Liverpool and the National Oceanography Centre, using data collected via the UK NERC-Defra Shelf Sea Biogeochemistry Program (Grants NE/K002007/1 and NE/K001701/1). The authors would like to acknowledge and thank Momme Butenschön (PML) for the SSB AMM7 configuration of the NEMO-ERSEM model, and Charlotte Williams (NOC) for the processed glider data (available at BODC at https://doi.org/10.5285/dd2a4f57-5943-68c7-e053-6c86abc0eb55). The authors would also like to thank the three anomalous reviewers whose constructive feedback helped significantly strengthen this manuscript.

References

Alexander, M. A., Kilbourne, K. H., & Nye, J. A. (2014). Climate variability during warm and cold phases of the Atlantic Multidecadal Oscillation (AMO) 1871–2008. *Journal of Marine Systems*, *133*, 14–26. https://doi.org/10.1016/j.jmarsys.2013.07.017

Behrenfeld, M. J. (2010). Abandoning Sverdrup's critical depth hypothesis on phytoplankton blooms. *Ecology*, *91*(4), 977–989. https://doi.org/10.1890/09-1207.1

Boss, E., & Behrenfeld, M. (2010). In situ evaluation of the initiation of the North Atlantic phytoplankton bloom. *Geophysical Research Letters*, *37*(18). https://doi.org/10.1029/2010gl044174

Butenschön, M., Clark, J., Aldridge, J. N., Allen, J. I., Artioli, Y., Blackford, J., et al. (2016). ERSEM 15.06: A generic model for marine biogeochemistry and the ecosystem dynamics of the lower trophic levels. *Geoscientific Model Development*, *9*(4), 1293–1339.

Chiswell, S. M. (2011). Annual cycles and spring blooms in phytoplankton: Don't abandon Sverdrup completely. *Marine Ecology Progress Series*, *443*, 39–50. https://doi.org/10.3354/meps09453

Chiswell, S. M., Bradford-Grieve, J., Hadfield, M. G., & Kennan, S. C. (2013). Climatology of surface chlorophyll a, autumn-winter and spring blooms in the southwest Pacific Ocean. *Journal of Geophysical Research: Oceans*, *118*(2), 1003–1018. https://doi.org/10.1002/jgrc.20088

Cohen, J., Screen, J. A., Furtado, J. C., Barlow, M., Whittleston, D., Coumou, D., et al. (2014). Recent Arctic amplification and extreme mid-latitude weather. *Nature Geoscience*, *7*(9), 627–637. https://doi.org/10.1038/ngeo2234

Collins, A. K., Allen, S. E., & Pawlowicz, R. (2009). The role of wind in determining the timing of the spring bloom in the Strait of Georgia. *Canadian Journal of Fisheries and Aquatic Sciences*, *66*(9), 1597–1616. https://doi.org/10.1139/f09-071

Cushing, D. H. (1974). The natural regulation of fish populations. In F. R. Harden Jones, (Ed.), *Sea Fisheries Research* (pp. 399–412). Elek Science.

Cushing, D. H. (1990). Plankton production and year-class strength in fish populations: An update of the match/mismatch hypothesis. *Advances in Marine Biology*, *26*, 249–293. https://doi.org/10.1016/s0065-2881(08)60202-3

D'Aleo, J. S., & Easterbrook, D. J. (2016). Relationship of multidecadal global temperatures to multidecadal oceanic oscillations. *Evidence-Based Climate Science*, 191–214. https://doi.org/10.1016/b978-0-12-804588-6.00011-2

Dee, D. P., Uppala, S. M., Simmons, A. J., Berrisford, P., Poli, P., Kobayashi, S., et al. (2011). The ERA-Interim reanalysis: Configuration and performance of the data assimilation system. *Quarterly Journal of the Royal Meteorological Society*, *137*(656), 553–597. https://doi.org/10.1002/qj.828

Delworth, T. L., Zhang, R., & Mann, M. E. (2007). Decadal to centennial variability of the Atlantic from observations and models. *Geophysical Monograph-American Geophysical Union*, *173*, 131.

Durant, J. M., Hjermann, D. Ø., Ottersen, G., & Stenseth, N. C. (2007). Climate and the match or mismatch between predator requirements and resource availability. *Climate Research*, *33*(3), 271–283.

Dye, S. R., Holliday, N. P., Hughes, S. L., Inall, M., Kennington, K., Smyth, T., et al. (2013). Climate change impacts on the waters around the UK and Ireland: Salinity. *MCCIP Science Review*, 60–66.

Edwards, K. P., Barciela, R., & Butenschön, M. (2012). Validation of the NEMO-ERSEM operational ecosystem model for the North West European Continental Shelf. *Ocean Science*, *8*(6), 983–1000.

Franks, P. J. (2015). Has Sverdrup's critical depth hypothesis been tested? Mixed layers vs. turbulent layers. *ICES Journal of Marine Science*, *72*(6), 1897–1907.

GEBCO. (2014). *The GEBCO_2014 Grid, version 20150318*. Retrieved from http://www.gebco.net

Gómara, Í., Rodríguez Fonseca, B., & Zurita Gotor, P. (2012). Explosive Cyclones in the North Atlantic: NAO Influence and Multidecadal Variability. *Publicaciones de la Asociación Española de Climatología. Serie A*, *8*.

Häkkinen, S., Rhines, P. B., & Worthen, D. L. (2011). Atmospheric blocking and Atlantic multidecadal ocean variability. *Science*, *334*(6056), 655–659.

Henson, S. A., Robinson, I., Allen, J. T., & Waniek, J. J. (2006). Effect of meteorological conditions on interannual variability in timing and magnitude of the spring bloom in the Irminger Basin, North Atlantic. *Deep Sea Research Part I: Oceanographic Research Papers*, *53*(10), 1601–1615.

Holt, J., & Umlauf, L. (2008). Modelling the tidal mixing fronts and seasonal stratification of the Northwest European Continental shelf. *Continental Shelf Research*, *28*(7), 887–903.

Holt, J., Wakelin, S., Lowe, J., & Tinker, J. (2010). The potential impacts of climate change on the hydrography of the northwest European continental shelf. *Progress in Oceanography*, *86*(3–4), 361–379.

Huisman, J., Jonker, R. R., Zonneveld, C., & Weissing, F. J. (1999). Competition for light between phytoplankton species: Experimental tests of mechanistic theory. *Ecology*, *80*(1), 211–222.

Ingleby, B., & Huddleston, M. (2007). Quality control of ocean temperature and salinity profiles— Historical and real-time data. *Journal of Marine Systems*, *65*(1-4), 158–175.

Jardine, J., Williams, C. A. J., & Palmer, M. R. (2022). *Slocum glider data from Units 345 ("Cabot"), 490 ("Fortyniner"), 397 ("Nelson") and 399 ("Rayleigh") in the Celtic Sea during the Shelf Sea Biogeochemistry Project, 2014–2015*. NERC EDS British Oceanographic Data Centre NOC. Accessed at: https://www.bodc.ac.uk/data/published_data_library/catalogue/10.5285/dd2a4f57-5943-68c7-e053-6c86abc0eb55

Körtzinger, A., Send, U., Lampitt, R. S., Hartman, S., Wallace, D. W., Karstensen, J., et al. (2008). The seasonal pCO2 cycle at 49 N/16.5 W in the northeastern Atlantic Ocean and what it tells us about biological productivity. *Journal of Geophysical Research*, *113*(C4).

Krueger, O., Feser, F., & Weisse, R. (2019). Northeast Atlantic storm activity and its uncertainty from the late nineteenth to the twenty-first century. *Journal of Climate*, *32*(6), 1919–1931.

Lacour, L., Ardyna, M., Stec, K. F., Claustre, H., Prieur, L., Poteau, A., et al. (2017). Unexpected winter phytoplankton blooms in the North Atlantic subpolar gyre. *Nature Geoscience*, *10*(11), 836.

Li, J., Sun, C., & Jin, F. F. (2013). NAO implicated as a predictor of Northern Hemisphere mean temperature multidecadal variability. *Geophysical Research Letters*, *40*(20), 5497–5502.

Luneva, M. V., Wakelin, S., Holt, J. T., Inall, M. E., Kozlov, I. E., Palmer, M. R., et al. (2019). Challenging vertical turbulence mixing schemes in a tidally energetic environment: 1. 3-D shelf-sea model assessment. *Journal of Geophysical Research: Oceans*, *124*(8), 6360–6387.

Madec, G. (2015). NEMO Ocean Engine. Retrieved from https://epic.awi.de/id/eprint/39698/1/NEMO_book_v6039.pdfhttps://epic.awi.de/id/eprint/39698/1/NEMO_book_v6039.pdf

Madec, G., Delecluse, P., Imbard, M., & Levy, C. (1997). Ocean general circulation model reference manual. *Note du Pôle de modélisation*.

Marshall, J., Kushnir, Y., Battisti, D., Chang, P., Czaja, A., Dickson, R., et al. (2001). North Atlantic climate variability: Phenomena, impacts and mechanisms. *International Journal of Climatology: A Journal of the Royal Meteorological Society*, *21*(15), 1863–1898.

Martin, A. P. (2003). Phytoplankton patchiness: The role of lateral stirring and mixing. *Progress in Oceanography*, *57*(2), 125–174.

Megann, A., Storkey, D., Aksenov, Y., Alderson, S., Calvert, D., Graham, T., et al. (2014). GO5.0: The joint NERC–Met Office NEMO global ocean model for use in coupled and forced applications. *Geoscientific Model Development*, *7*(3), 1069–1092.

Mölter, T., Schindler, D., Albrecht, A. T., & Kohnle, U. (2016). Review on the projections of future storminess over the North Atlantic European region. *Atmosphere*, *7*(4), 60.

O'Dea, E. J., Arnold, A. K., Edwards, K. P., Furner, R., Hyder, P., Martin, M. J., et al. (2012). An operational ocean forecast system incorporating NEMO and SST data assimilation for the tidally driven European North-West shelf. *Journal of Operational Oceanography*, *5*(1), 3–17.

O'Dea, E. J., Furner, R., Wakelin, S., Siddorn, J., While, J., Sykes, P., et al. (2017). The CO5 configuration of the 7 km Atlantic Margin Model: Large-scale biases and sensitivity to forcing, physics options and vertical resolution. *Geoscientific Model Development*, *10*(8), 2947–2969.

Pingree, R. D., Holligan, P. M., Mardell, G. T., & Head, R. N. (1976). The influence of physical stability on spring, summer and autumn phytoplankton blooms in the Celtic Sea. *Journal of the Marine Biological Association of the United Kingdom*, *56*(4), 845–873.

Platt, T., Fuentes-Yaco, C., & Frank, K. T. (2003). Marine ecology: Spring algal bloom and larval fish survival. *Nature*, *423*(6938), 398.

Poulton, A. J., Davis, C. E., Daniels, C. J., Mayers, K. M., Harris, C., Tarran, G. A., et al. (2019). Seasonal phosphorus and carbon dynamics in a temperate shelf sea (Celtic Sea). *Progress in Oceanography*, *177*, 101872.

Schlesinger, M. E., & Ramankutty, N. (1994). An oscillation in the global climate system of period 65–70 years. *Nature*, *367*(6465), 723.

Sharples, J., Holt, J., & Dye, S. R. (2013). Impacts of climate change on shelf sea stratification. *MCCIP Science Review*, 67–70.

Sharples, J., Mayor, D. J., Poulton, A. J., Rees, A. P., & Robinson, C. (2019). Nutrient and carbon cycling in a temperate shelf sea water column. *Progress in Oceanography*, *177*, 102182.

Sharples, J., Ross, O. N., Scott, B. E., Greenstreet, S. P., & Fraser, H. (2006). Inter-annual variability in the timing of stratification and the spring bloom in the North-western North Sea. *Continental Shelf Research*, *26*(6), 733–751.

Siddorn, J. R., & Furner, R. (2013). An analytical stretching function that combines the best attributes of geopotential and terrain-following vertical coordinates. *Ocean Modelling*, *66*, 1–13.

Siegel, D. A., Doney, S. C., & Yoder, J. A. (2002). The North Atlantic spring phytoplankton bloom and Sverdrup's critical depth hypothesis. *Science*, *296*(5568), 730–733.

Simpson, J. H., & Bowers, D. (1981). Models of stratification and frontal movement in shelf seas. *Deep Sea Research Part A. Oceanographic Research Papers*, *28*(7), 727–738.

Simpson, J. H., & Hunter, J. R. (1974). Fronts in the Irish sea. *Nature*, *250*(5465), 404–406.

Sommer, U., & Lengfellner, K. (2008). Climate change and the timing, magnitude, and composition of the phytoplankton spring bloom. *Global Change Biology*, *14*(6), 1199–1208.

Sverdrup, H. U. (1953). On conditions for the vernal blooming of phytoplankton. *ICES Journal of Marine Science*, *18*(3), 287–295.

Taylor, J. R., & Ferrari, R. (2011). Shutdown of turbulent convection as a new criterion for the onset of spring phytoplankton blooms. *Limnology & Oceanography*, *56*(6), 2293–2307.

Townsend, D. W., Cammen, L. M., Holligan, P. M., Campbell, D. E., & Pettigrew, N. R. (1994). Causes and consequences of variability in the timing of spring phytoplankton blooms. *Deep Sea Research Part I: Oceanographic Research Papers*, *41*(5–6), 747–765.

Townsend, D. W., Keller, M. D., Sieracki, M. E., & Ackleson, S. G. (1992). Spring phytoplankton blooms in the absence of vertical water column stratification. *Nature*, *360*(6399), 59.

Visbeck, M. H., Hurrell, J. W., Polvani, L., & Cullen, H. M. (2001). The North Atlantic Oscillation: Past, present, and future. *Proceedings of the National Academy of Sciences of the United States of America*, *98*(23), 12876–12877.

Vörösmarty, C. J., Fekete, B. M., Meybeck, M., & Lammers, R. B. (2000). Global system of rivers: Its role in organizing continental land mass and defining land-to-ocean linkages. *Global Biogeochemical Cycles*, *14*(2), 599–621.

Weisse, R., Von Storch, H., & Feser, F. (2005). Northeast Atlantic and North Sea storminess as simulated by a regional climate model during 1958–2001 and comparison with observations. *Journal of Climate*, *18*(3), 465–479.